Full Length Research Paper

Electrical Resistivity Imaging (ERI) of basin fills in some parts of Eastern Dahomey

Akinmosin A. A.[1], Omosanya K. O.[2,3]*, Ikhane P. R.[2], Mosuro G. O.[2] and Adetoso A. O.[1]

[1]Department of Geoscience, University of Lagos, Akoka
[2]Department of Earth Sciences, Olabisi Onabanjo University, Ago-Iwoye, Nigeria
[3]Cardiff University, School of Ocean, Earth and Planetary Science, United Kingdom

Stratigraphic and geophysical analyses of an outcrop at Onikintibi were done with the aim of understanding basin architecture and predicting depositional history. The palynological studies defined the age of the units, and clarified the lithology of the basal component. Three principal lithology types found are conglomeratic sands, compacted ferruginised sandstone, and the weathered basement; these units have resistivity values of >1000 Ωm, >1019Ωm and <400Ωm. The basal layer is derived from porphyritic granite protolith. In addition, coarsening-upward stacking pattern of the reddish-brown conglomerate suggests prevalence of continental conditions. High thickness of the Ise units at the western edge suggests greater accommodation space and subsidence during basin development; consequently, the layer tapers to the east in response to waning current. The occurrence of Monoporites annulatus, Laevigatosporites and Acrostichum aureum imply the outcrop is post Paleocene. Longapertites sp. is an extant plant taxa with known ecological preferences assigned to Nypa (a mangrove plant), thus vegetation comparable to Nypa mangrove may have occurred in the region. The lithologic units over the weathered basement are rocks of the Abeokuta group in Eastern Dahomey Basin.

Keywords: Dahomey, basin, resistivity, palynology, Ise.

INTRODUCTION

The growth of sedimentary basins is controlled by the interplay of tectonism, sediment supply, sea level condition, erosion, and subsidence (Lambiase and Bosworth, (1995), Schlische, (1991), Rosendahl, (1987), Vail et al., (1977), Van Wagoner et al., (1990)). The geometry of a basin can provide clues to conditions prevalent during its evolution; such information may include the volume and amount of sediment transported, degree of deformation related to tectonism, character of transporting medium, proximity of sediment source area, etc., lithological and biological information derived from the rock record are the invaluable tools for effective basin analysis.

The geologic examination of basin architecture relied on analysis of gravity, magnetic and seismic reflection data (Hole et al., (2011), Unsworth et al., (1999)); electrical method had little use for such investigation as it is limited to shallow depth investigation. Resistivity technique, however, is appropriate for the evaluation of groundwater potential, hydrocarbon exploration (bitumen), foundation investigation, mapping of underground contaminants, soil properties, geology and subsurface (Batayneh et al., (2004), Boadu et al., (2005), Sirhan et al, (2011), Ikhane et al., (2011), Yunus et al, 2008, Ehirim and Ofor, (2011), Majumdar and Das, (2011), Nwankwo, (2011), Leucci, (2006), Skjernaa and Jorgensen, (1993), Al-Hagrey, (1994); Molindo and Alile, (2007)).

Advances in electrical resistivity imaging have made it possible to extend shallow geophysical investigations in two and three-dimensional images (Colella et al, (2004), Steeples, (2001), Suzuki et al., (2000)). Appropriately planned survey lines can yield 3D images, geometries and greater depth of investigation useful for effective basin study. In addition, biostratigraphy analysis can provide invaluable information on the age of the units.

*Corresponding Author E-mail:kamaloomosanya@yahoo.com
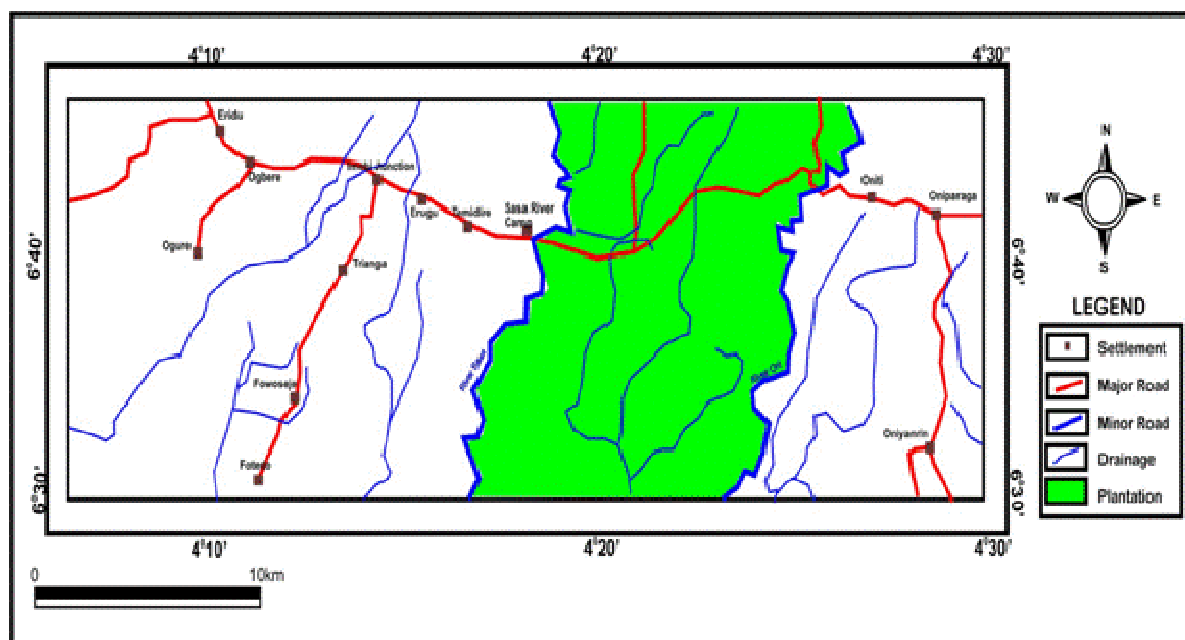
Figure 1. Index map of the study area (Onikitibi)

Stratigraphic palynology has been used to date rocks of Precambrian to Recent; it involves the analysis of contemporary and fossil palynomorphs, including pollen, spores, dinoflagellate cysts, architarchs, chitinozoans and scolecodont, together with particulate organic matter (POM) and kerogen found in sediments and sedimentary rocks. Palaoenvironment reconstruction using palynomorphs relies on the abundance of these organisms today, which is an indication of environmental variables that controlled their distributions. Palynomorphs are abundant, easily preserved, and closely correlated with local environments.

The thrust of this research is to use electrical resistivity and palynological techniques to picture geometry of an outcrop and also reconstruct its evolutionary history. In this paper, we start by discussing the regional geology and stratigraphy of the area, methods adopted for the research; discussion of the results from the field and integration results from the different techniques.

Regional geologic setting and stratigraphy

The Benin (Dahomey) Basin constituted part of a system of the West African peri-cratonic (margin sag) basin (Klemme (1975); Kingston et al (1983)) developed during

The lithostratigraphic units of the eastern margin of Dahomey basin is summarized in Table 1. The study area belongs to the Cretaceous Abeokuta group; the oldest group of sediment unconformably overlying the basement (Jones and Hockey, 1964). Omatsola and

the commencement of the rifting associated with the opening of the Gulf of Guinea in the Early Cretaceous to the Late Jurassic (Burke et al, (1971); Whiteman, (1982)). The crustal separation naturally was preceded by crustal thinning and accompanied by an extensive period of thermally induced basin subsidence during early Cretaceous to Tertiary times as the South American and the African plates entered a drift phase to accommodate the emerging Atlantic Ocean (Storey,(1995); Mpanda, (1997)).

The Ghana Ridge, presumably an offset extension of the Romanche Fracture Zone, binds the basin to the west while the Benin Hinge Line, a Basement escarpment which separates the Okitipupa Structure from the Niger Delta basin binds it to the east. The Benin Hinge Line supposedly defines the continental extension of the Chain Fracture Zone. The onshore part of the basin covers a broad arc-shaped profile of about 600km^2 in extent. The onshore section of the basin attains a maximum width, along its N-S axis, some 130 km around the Nigerian – Republic of Benin border. The basin narrows to about 50km on the eastern side where the basement assumes a convex upwards outline with concomitant thinning of sediments. Along the northeastern fringe of the basin where it rims the Okitipupa high is a brand of tar (oil) sands and bitumen seepages (Nwachukwu and Ekweozor, 1989)).

Adegoke (1981) recognized three (3) Formations in the Abeokuta group based on lithologic homogeneity and similarity of provenance. The Abeokuta group is the thickest sedimentary unit in the area and includes rocks of the Ise, Afowo and Araromi formation.

Table 1. Stratigraphic units of Eastern Dahomey Basin.

Jones and Hockey(1964)			Omatsola and Adegoke (1981)		Agagu (1985)	
	Age	Formation	Age	Formation	Age	Formation
Quaternary	Recent	Alluvium			Recent	Alluvium
Tertiary	Pleistocene-Oligocene	Coastal Plain Sand	Pleistocene-Oligocene	Coastal Plain Sand	Pleistocene-Oligocene	Coastal Plain Sand
	Eocene	Ilaro	Eocene	Ilaro	Eocene	Ilaro
	Palaeocee	Ewekoro	Palaeocene	Oshosun Akinbo Fm	Palaeocene	Oshosun Akinbo Ewekoro
Cretaceous	Late Senonian	Abeokuta	Maastrichtian-Neocomian	Araromi Afowo Ise	Maastrichtian-Neocomian	Araromi Afowo Ise
			Precambrian Crystalline Basement Rocks			

The Ise formation unconformably overlies the basement complex in south western Nigeria; it consists of conglomerates and grits at the base which is in turn is overlain by coarse to medium grained sands interbeded with kaolinite. The conglomerates are imbricated, at some locations they were associated with ironstones (Nton, 2001). Based on paleontological assemblages, age range of Neocomian-Albian is assigned to this formation. In addition, the Afowo formation overlies the Ise, and is composed of coarse to medium grained sandstone with variable but thick interbedded shale, siltstone and claystone. The sandy facies is tar-bearing while the shales are organic-rich (Enu, 1995). Based on palynological assemblage, a Turonian age is assigned to the Lower part of this formation, while the upper part ranges into Maastrichtian. The youngest Formation in the Abeokuta group is Araromi, which conformably overlies the Afowo formation. The Formation is composed of fine-medium grained sandstone, shales, silt-stone with interbedded limestones, marl and lignite. Based on preserved faunal content, Omatsola and Adegoke (1981) dated the Araromi Formation Maastrichtian-Paleocene.

The Abeokuta group is overlain by the Imo group composed of Ewekoro and Akinbo Formation (Adegoke, (1977), Jones and Hockey, (1964), Ogbe, (1972), Nton and Elueze, (2005), Nton (2001); Oshosun formation (Jones and Hockey, (1964); Nton, (2001)); Coastal plain sands and the Recent Alluvium (Jones and Hockey, 1964).

METHODOLOGY

The approaches used in this work include geological mapping, geophysical survey and laboratory analysis for the palynomorphs.

Geological Mapping

Lithologic description of a subcrop closest to the geoph-ysical survey line was in order to tie geology with the pseudosections. Parameters estimated include: the lithology type, textural characteristics, sedimentary structures, color, attitude (strike and dip) and thickness. The latter was measured to a local datum of 1.7m from the base of the ditch. A cross section line ~15m in length was drawn with lithological logs at 0, 3, 6, 9, and 15m from west to east. Samples were chosen based on physical similarity, nine (9) samples were collected, three (3) from each of the position 0, 6 and the 15m. They were bagged in polythene bags and labeled for subsequent laboratory analysis.

Geophysical Survey

Electrical imaging was done using Wenner electrode configuration; for this purpose, three (3) profile lines of 100m long were chosen along the exposures in the east west direction, they were separated 20m apart in the N-S direction forming a grid 60m x 100m. A current of 5mA was introduced into the ground whilst the terrameter was set to average the resultant resistivity over a cycle of 4. As the distance between the current electrodes is progressively increased, the potential electrode (P) remained unchanged until the voltage becomes too small to measure; at distance of AB/2 > 350m the current was increased to 10mA, and the P separation increased in order to be moved between successive readings. The electrode spacing between the adjacent electrode was assigned "a." For a system with 20 electrodes, there are (20-(1x3)), (20-(2x3), (20-(3x3), (20-(4x3) possible measurements for "1a," "2a," "3a," "4a" electrode spacing respectively and so on. This implies that, as the electrode spacing increases, the number of measurement decreases. The first procedure was to carry out all the possible measurements for the Wenner array with electrodes spacing of "1a." For the first measurement, electrodes number 1, 2, 3 and 4 were used. Electrode 1 was used as the first current electrode (C_1), electrode 2 as the first potential electrode (P_1), electrode 3 as the

second potential electrode (C_2) and electrode 4 as the second current electrode. For the second measurement, electrodes number 2, 3, 4 and 5 were used for C_1, P_1, P_2 and C_2 respectively. This was repeated down the lines of electrodes until electrodes 17,18,19,20 are used for the last measurement with "1a" spacing for Wenner array. After completing the sequence of measurement with "1a" spacing, the next sequence of measurement with "2a" was made. Firstly, electrodes number 1, 3, 5 and 7 were used for the first measurement. The electrodes were chosen so that the spacing between the adjacent is "2a" for the second measurement; electrodes 2, 4, 6 and 8 were used. This process was repeated down the last measurement with spacing "2a." The same process was done for measurements with "3a," "4a," "5a"and "6a" spacing respectively; with a spacing of 5, 10, 15,20,25, and 30, the survey was done with the practical assumption that depth of 3,6, 9,12, 15, and 18 m (depth = ~0.6 of electrode spacing) were being investigated.

Interpretation of the field data was done using RES2DINV ver 3.55 software; the apparent resistivity was determined from the product of resistance and the geometric factor for Wenner configuration. Furthermore, smooth and robust inversions were done to compare the results and detect sedimentary boundaries. The inversion process is iterative, and useful for creating resistivity models of the subsurface. A starting model was chosen based on a-priori information from ground truth or averaged geophysical measurements; apparent resistivity data was modeled according to the survey geometry. The calculated data were compared with the field measurements; the model was updated to accommodate the difference between the observed and estimated results. This procedure was repeated until the derived data match the actual readings to within an interpreter-defined level of error. The consequence of the inversion process is a better estimate of depth for cross-section plots, which turns pseudo-sections into reliable approximations of the subsurface variation.

Laboratory (Palynological) Analysis

The nine (9) samples from litho description were analysed at Mosunmolu Palaeontology laboratory; they were subjected to different kinds of treatments prior to analysis under the microscope, which include (i)Treatment with Dilute HCL; in order to remove any carbonate material usually calcite in the sample, the samples were mixed with hydrochloric acid (HCl), carbonates generally effervesces in the presence of HCl acid (ii) Digestion of the sample; 60% Hydrofluoric acid (HF) was added to the samples earlier treated, with the samples soaked overnight and stirred intermittently with a plastic rod in order to achieve maximum digestion. The supernatant liquid was decanted gently, and the substrate rinsed with distilled water. (iii) Sieving, samples

were sieved with 5-10μ in order to remove the clayey materials from it. (iv) Oxidation, drops of HNO_3 were put in the residue in order to bleach it; the reaction was stopped by the addition of Potassium Hydroxide (KOH) (v) Heavy Liquid Separation, Zinc chloride ($ZnCl_2$) was added to sets of test tubes containing the residue, and the amount of liquid in each of the test tubes was measured to the same level before they were placed in the centrifuge. The centrifuge was adjusted to a revolution of 2000 per minute for 15 minutes to achieve effective separation. The organic matter with specific gravity less than 2.2 gcc^{-1} floated while those heavier than 2. 2gcc-1 settled to the bottom of the tube. The floated material was carefully decanted into a clean tube and labeled without allowing the mixture with the heavy materials at the bottom of the tube. The collected organic residue was rinsed with distilled water. (vi)Treatment with Alcohol, the residues were rinsed with ethanol before being mounted on the slides in order to achieve permanent slide preparation. The ethanol will remove any water trapped within the organic residue.(vii) Final Slide Mounting, the ethanol-rinsed residue was placed on a covered slip on a hot plate. The residue was spread over it and allowed to dry up. After this, drop of mountant liquid was instantly dropped on the glass slide, spread to approximately the size of the cover slip. This was quickly mounted on the cover slip, spread out with the finger in order to expel any oxygen that might have been trapped during the mounting of the cover slip. The slides were allowed to dry for ~2days and were studied under the microscope.

RESULTS AND DISCUSSION

Lithologic description

Three (3) rock types were identified in the subcrop; they include conglomeratic sand (Figure 2 and 3) composed of red sandstones and very angular clasts of feldspars and quartz. The unit grades into less coarse sands from west to eastern part of the exposure. A thin lineation of conglomerate pebbles separates the red from brown conglomeratic argillaceous sand/sandstone; the lineation dips approximately $<2^0$ E. Beneath this sedimentary marker is medium-coarse grained brownish conglomeratic clayey-sandstone (Figure 2 and 3) which becomes progressively finer towards the base. The basal unit is clayey and characterized by highly eroded feldspar clasts derived from alteration of probable porphyritic granite. The sequence is chronologically clayey/weathered basement, brown conglomeratic sand, conglomerate pebbles and reddish conglomeratic sandstone. Thickness of the beds increases to the west which suggests greater accommodation space and subsidence of the basin during deposition. In contrast, the units thin out to the east as velocity of the
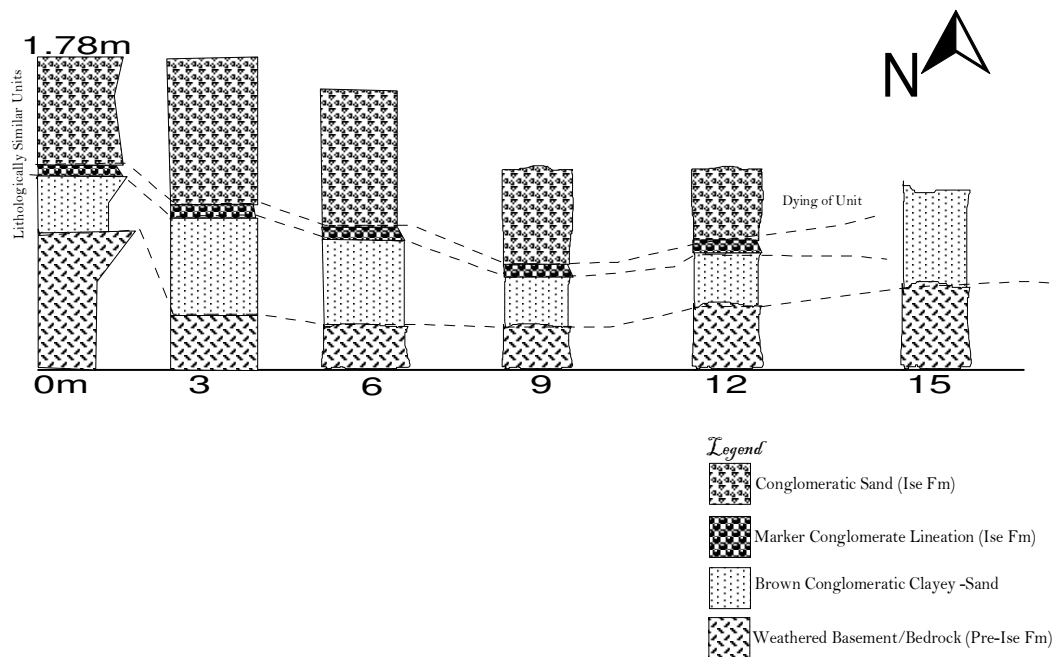
Figure 2. The Lithology Correlation of the lithosections during the Geological Mapping

Figure 3. (a)The subrounded clasts of the conglomeratic sandstone mapped at the uppermost part of the subcrop (b) Extension of the uppermost layer (c) first arrow points to the conglomeratic sands, second to the brown conglomeratic clayey sand and the third to the weathered basement rock. (d) Arrow point to the conglomerate lineation.

transporting medium wanes, making the beds to onlap onto the basement. Correlation of the exposure to the west shows that the unit above the weathered basement bears characteristics of the Ise Formation (see Figure 2).
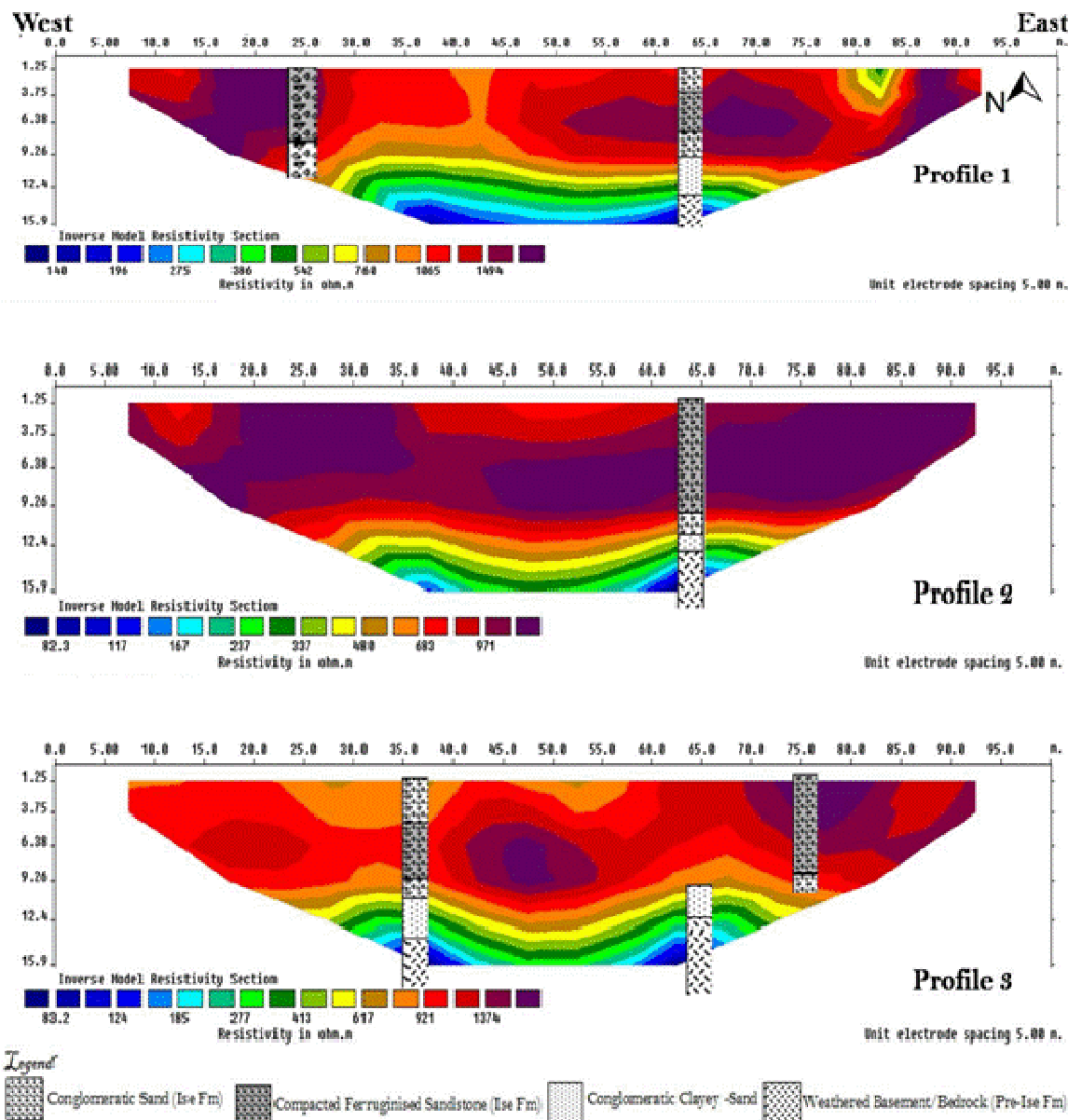
Figure 4. The smooth inverted resistivity Pseudosection along Profile 1, 2 and 3.

The color of sedimentary rock is an indicator of the environment of deposition; red color is synonymous with terrestrial environment, brown to transitional and black and gray to deep marine environment of deposition. The reddish conglomerate sands were deposited in a continental basin with iron oxide as the principal cement. Consequently, the brown conglomerates are marginal; additionally, the coarsening upward pattern is reflective of beach sands or swamps.

Resistivity Pseudosection

In Figure 4 the lithology identified from profile 1 include

conglomeratic sands (CS) with resistivity of 386 - <1065 Ωm, compacted ferruginised sandstone (CFS), >1065Ωm, and weathered basement (WB) rock with resistivity value of <386Ωm. In contrast, the robust inverted pseudosection shows the dominance of CFS, with resistivity values of >1249Ωm from the surface to depth ~12. 4m, the other rock type includes the CS and WB rock with resistivity value of ~354-<1249Ωm and < 354Ωm respectively. Both sections show that some of the CS is sandwiched by the CFS to the east of the profile line. For profile 2, both the smooth and robust inverted pseudosection show a succession of CS with resistivity value of >852Ωm, CFS between >337- <852Ωm, and WB rock of <337Ωm. At the uppermost part of the both
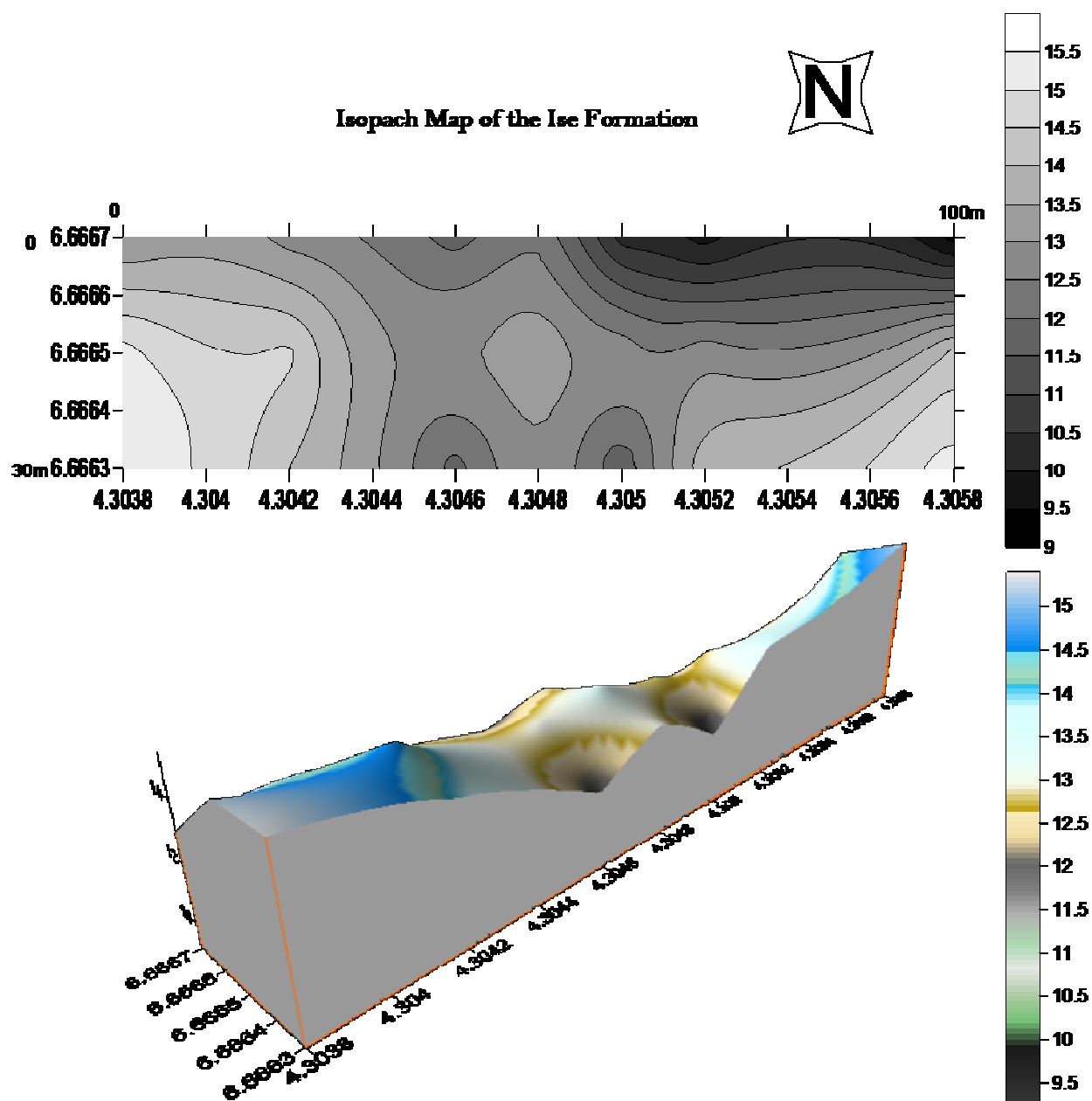
Figure 5. Isopach Map and cross section of the Ise Formation above the weathered basement

pseudosection, the CS is sandwiched by the CFS. The CS is predominant at the western to central uppermost part of the pseudosection in profile 3, occurring to depth of ~ 12.4m on the smooth and ~5.00m on the robust inverted pseudosection. The CFS occurs at the eastern uppermost part to depth of <9. 26m, however, on the robust pseudosection, it is the dominant lithology from depth of ~3.75-11.0m. The resistivity of the rock types are > 1019Ωm, >277Ωm - <1019 Ωm and < 277Ωm for CFS, CS and WB respectively.

From the pseudosections (Figure 4), three principal (3) lithology types were identified, which include the conglomeratic sands, compacted ferruginised sandstone and the weathered basement with resistivity values that ranges between 150->1000 Ωm, >1019Ωm and less than 400Ωm respectively. The basement rock from field observation is composed of eroded clast of feldspar suggesting that the initial rock was derived from porphyritic granite or Porphyroblastic gneiss; the degree of weathering is intense and the rock equivocally resembles a mudstone. There is no preferred orientation of the weathered feldspars fragments which implies lack of structural attitude (i.e. strike) buttressing the origin of the basement to be igneous.
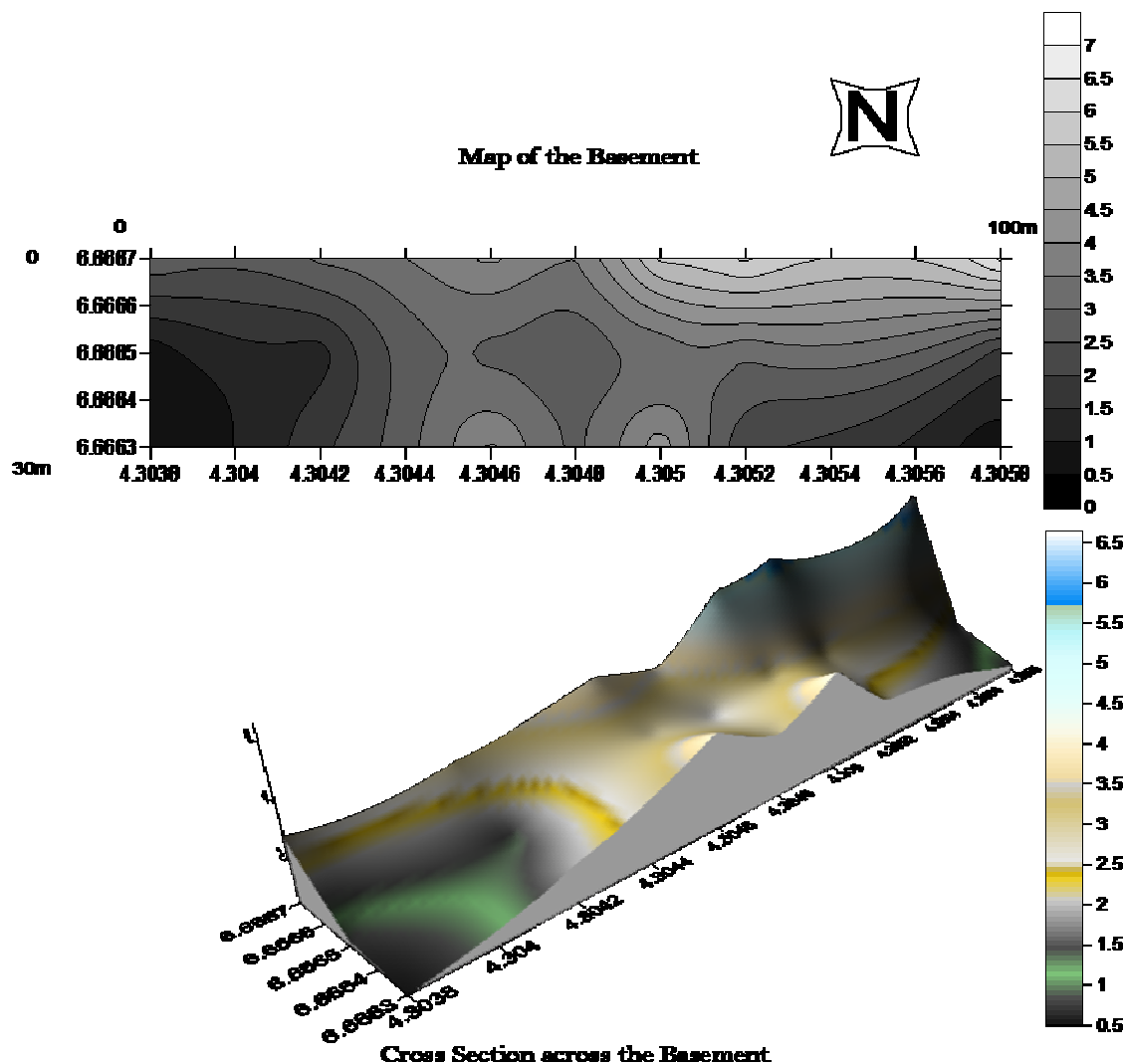
**Figure 6.** Map and Cross Section through the Weathered Basement.

In order to understand the depositional trend vis-à-vis accommodation space and sediment supply, the unit above the weathered basement was considered as a single Formation, the geological models built from Figure 4 were used to estimate the thickness of the layers, and where no data exists the layers were extrapolated. The model entails that (1) the compacted ferruginised sandstone (CFS) is impregnated in the conglomeratic sands (CS), evidence from pseudosection (Figure 4) and field observations (Figure 2 and 3) that the rock is Detrital and was derived from different parent materials. (2) The weathered basement is characterized by a depression at the 50m point on resistivity profile 2 and 3, and also bounded by basement highs to the west and east.

The robust inversion shows that the unit above the basement is characterized by high resistive rock, the compacted ferruginised sandstone, and that the geometry of the basement differs from profile 1-3; the basement is imaged as a flat surface on Profile 3. Overall, the Ise Formation consists of the conglomeratic sands and ferruginised sandstone with resistivity value of >300 Ωm - >1300Ωm and thickness of 9.26 to 15. 4m; mean thickness of Ise in the study area is ~12. 86m. Volume of sediment deposited in the area, therefore, is approximately 77160m3 (0.0008km3), from the product of the profile length, separation between lines (N-S) and the average thickness.

Isopach map of the Ise Formation (sensu the conglomeratic sands and compacted ferruginised sandstone) was produced to inferr conditions of basin development such as subsidence and uplift; this exercise provided information on the depositional pattern and clues on area of variable stratigraphic thickness, and those affected by faults or other kind of deformation. The Isopach map displays the thickness of the Ise to the top of the weathered basement, while the topography for the
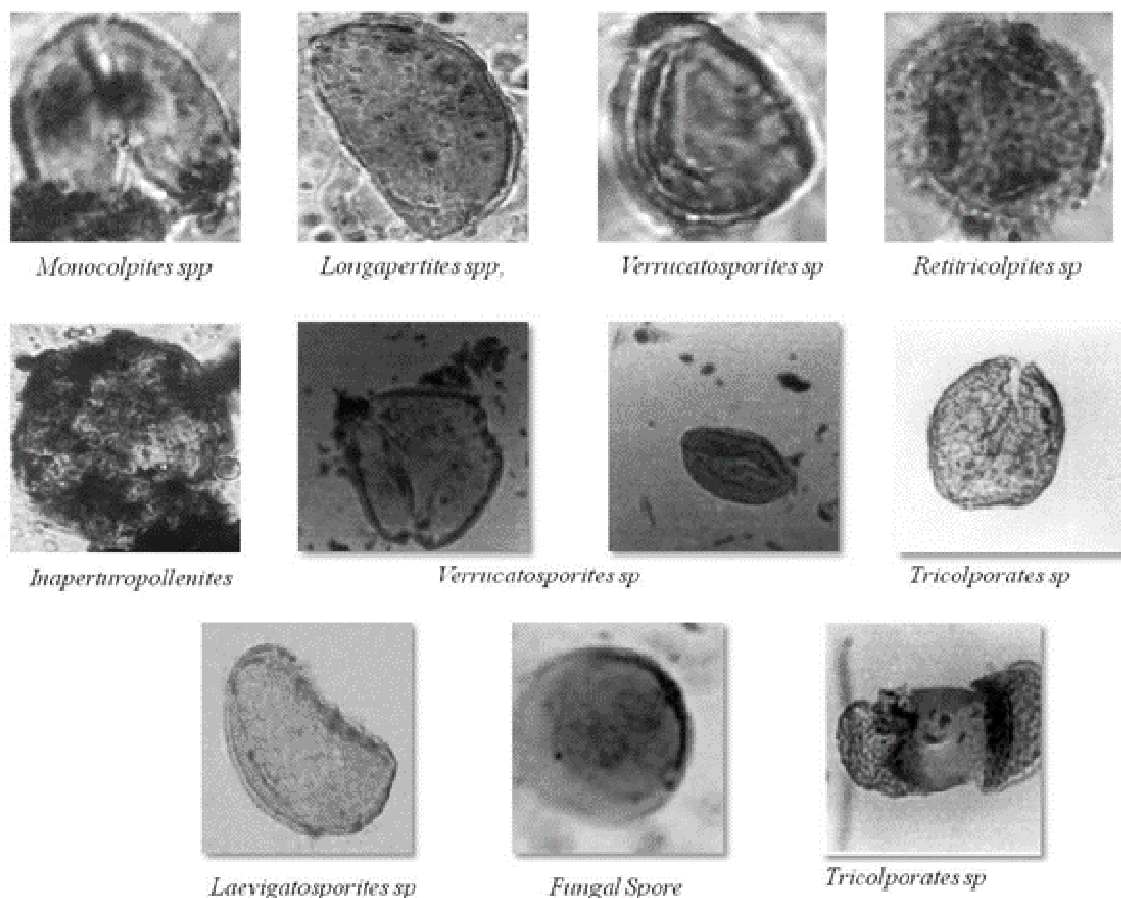
Figure 7. Some of the palynomorphs species found in the study area.

basal unit was estimated from the difference of the thickness of Ise Formation from the depth of imaging shown on pseudosections.

In Figure 5 and 6, the Formation is thicker at the west and eastern edges but thin at the centre, where it coincides with the position of the basement high. Subsidence is a product of either thermal reaction within the mantle (thermal subsidence, Bott 1979 and 1982) or as a result of extension of the crust (fault-controlled subsidence, Kusznir and Ziegler, 1992, Whiteand Mc kenzie, 1989). Basement high at the centre implies lesser accommodation space, higher deposition is commensurate with larger accommodation space and vice versa, which implies that more sediments are deposited to the west and east while fewer are deposited in the centre. Thus, subsidence is greater at the extreme while uplift is dominant at the centre; in addition, elevated sediment bypass may be recorded at the centre than the flanks.

Palynological Studies

The samples contain poor abundance and diverse pal

palynomorphs. The palynomorphs found in the area include Spores (Psilatricolporites, Laevigatosporites), Gynosperm pollen (Inaperturopollenites sp), Angiosperm Pollen (Longapertites sp, Tricolporates sp, Retritricolporites) and fungal spores. The highest occurrence of species recorded is of Laevigatosporites in a sample B3 followed by Acrostichum aureum and Monoporites annulatus.

The few occurrences of Monoporites annulatus, Laevigatosporites and Acrostichum aureum suggest age from late Paleocene to Recent. Longapertites sp. is an extant plant taxa with known ecological preferences which is assigned to Nypa, a mangrove plant (Germeraad et al,1968). Nypa fruits are known in the area from the early Tertiary (Gregor and Hagn, 1982), thus, vegetation comparable to Nypa mangrove may have occurred in the region, and the contemporary palaeoclimate was probably tropical-humid (Schrank, 1991). The presence of Longapertites spp, Tricolporates spp, Monocolpites spp which are index fossils that characterize early Maastrichtian age compare favorably with previous works of Lawal, 1982; Lawal and Moullade, 1986; Edet and Nyong 1994; and Ogala et al., 2009, Jones and Hockey (1964) and Adegoke and Omatsola (1981). Rare

Table 2. Distribution of Palynomorphs in the study Area

Formation	Units	Thickness(cm)	Palynomorphs	Count	Age	Abundance
Ise Fm	A0	96	Verrucatosporites sp	2	Palaeocene-Maastrichtian	Common
			Psilatricolporites	1		Common
			Laevigatosporites sp	2		Common
			Psilatricolporites crassus	2		
Marker Bed		10	-	-		
Ise Fm	B0	17	Barren			
Weathered Basement	C0	-	Fungal spores	1	Early Maastrichtian	Single
			Monocolpites sp	1		"
			Longapertites sp	1		"
Ise Fm	A3	100	Fungal spores	1	Palaeocene-Maastrichtian	
			Laevigatosporites sp	1		
			Tricolporates sp	1		
Marker Bed		8	-	-		
Ise Fm	B3	20	Monoporites annulatus	3	Palaeocene-Maastrichtian	
			Laevigatosporites sp	4		
			Fungal spores	1		
			Retitricolporites sp	1		
			Acrostichum aureum	1		
			Zonocostites ramonae	1		
			Inaperturopollenites sp	1		
Weathered Basement	C3	-	Laevigatosporites sp	2	Indeterminate	
			Tricolporates sp	1		
			Fungal spores	1		
Ise Fm	A6	98	Acrostichum aureum	3	Palaeocene-Maastrichtian	
			Inaperturopollenites sp	1		
			Verrucatosporites sp	2		
			Zonocostites ramonae	2		
			Fungal spores	1		
Marker Bed		8	-	-		
Ise Fm	B6	28	Fungal spores	1	Early Maastrichtian	
			Longapertites sp	1		
			Laevigatosporites sp	1		
Weathered Basement	C6	-	Laevigatosporites sp	1	Indeterminate	
			Monocolpites sp	1		
			Verrucatosporites sp	1		

mangrove specie Zonocostites ramonae with rainforest taxon Psilatricolporites crassus indicate a probable wet period occurring with episodes of a dry period (indicated by presence of Monoporites annulatus)

CONCLUSION

The study area lies within the eastern part of Dahomey basin in southwestern Nigeria; the exposure seen by the ditch showed three distinct lithologies: conglomeratic sands, compacted ferruginised sandstone both of the Ise Formation overlying the weathered basement complex of protolithic porphyritic granite. General thickening of the units in the west and thinning towards the east implies a greater accommodation space for sediment towards the west and lesser amount of sediments east. Basement high at the centre is related thermal subsidence (Storey, 1995) than tectonic fracturing. Contemporary palaeoclimate was probably tropical-humid climate due to the presence of Nypa mangrove species, rare man-grove specie Zonocostites ramonae with rainforest taxon

Psilatricolporites crassus indicate a probable wet period occurring with episodes of dry period. Commercial hydrocarbon or water can find in regions of higher accommodation spaces with groundwater flow being highest in this direction. Multiple two dimensional ERI data is a reliable means of generating three dimensional resistivity image of the subsurface.

ACKNOWLEDGEMENT

REFERENCES

Adegoke OS (1977). Stratigraphy and Paleontology of the Ewekoro Formation (Paleocene) of Southwestern Nig. Bull. Am. Palaeontol., Vol. 71, No. 295, 357pp.

Adegoke OS, Ako BD, Enu EI (1980). Geotechnical Investigations of the Ondo State bituminous sands Vol. 1. Geology and Reserves Estmate. Unpub. Rept., Geological Consultancy Unit, Department of Geology, University of Ile-Ife, 257pp.

Agagu OK (1985). A geological guide to bituminous sediments in Southwestern Nigeria. Unpubl. Report, Department of Geology, University of Ibadan.

Ajayi TR, Oyawale AA, Islander FA , Asubiojo OI, Klein DE, Adediran AI (2006). Trace and Rare Earth Elements Geochemistry of Oshosun Sediments of Dahomey Basin, Southwestern Nigeria. J. App. Sci. 6: 2067-2076.

Batayneh AT, Abdallah S, Al-Zoubi M, Abu-Ajamieh M (2004). Geoelectrical Soundings and their Relationship to Channel Seepage Areas at the Kaffrein Dam, Jordan. J. Appl. Sci. 4: 28-37.

Bott MHP (1979). Subsidence mechanisms at passive continental margins. American Association of Petroleum Geologists Memoir 29, 8-19

Bott MHP (1982). The mechanism of continental splitting. Tectonophysics 81, 301-309.

Burke KCB, Dessauvagie TFJ, Whiteman AJ (1971). The opening of the Gulf of Guinea and the geological history of the Benue depression and Niger Delta. Nature Physical Science 233 (38), 51–55.

Colella A, Lapenna V, Rizzo E (2004). High-resolution imaging of the High Agri Valley Basin (Southern Italy) with electrical resistivity tomography. Tectonophysics 386, 29-40.

Edet JJ, Nyong EE 1994). Palynostratigraphy of Nkporo shale exposure, Late Campanian-Maastrichtian on the Calabar flank, S.E. Nigeria. Rev. of Paleobot. And Palynology. Elsevier science. nmAmst. Vol. 80, pp. 131-147.

Ehirim CN, Ofor W (2011). Assessing Aquifer Vulnerability to Contaminants near Solid Waste Landfill Sites in a Coastal Environment, Port Harcourt, Nigeria. Trends in Applied Sciences Research, 6: 165-173.

Enu EI (1985). Textural characteristic of the Nigerian Tar Sands. Sedimentary geology. Vol. 44, pp. 65-81.

Giovanni L (2006). Integrated Geophysical, Geological and Geomorphological Surveys to Study the Coastal Erosion. International Journal of Soil Science, 1: 146-167.

Hole JA, Catchings RD, St Clair KC, Rymer MJ, Okaya DA, Carey BJ (2001). Steep-dip seismic imaging of the shallow San Andreas fault near Parkfield. Science 294, 1513-1515.

Jones HA, Hockey RD (1964). The geology of part of southwestern Nigeria. Geological Survey of Nigeria (GSN) Bulletin 31, 101.

Kusznir NJ, Ziegler PA (1992). The mechanics of continental extension and sedimentary basin formation: a simple-shear/pure-shear flexural cantilever model. Tectonophysics 215, 117-131.

Lambiase JJ, Bosworth, W (1995). Structural controls on sedimentation in continental rifts, in Lambiase, J.J., ed., Hydrocarbon habitat in rift basins: Geological Society Special Publication 80, p. 117-144.

Lawal OA (1982). Biostratigraphie palynologique es paleoenvirumens des formations Cretacee de la Haute-Benoue, Nigeria mord-orietal. These-3-cycle, Univ. Nice, 218pp.

Lawal OA, Oullade M (1986). Palynological biostratigraphy of some Cretaceous sediments in the Upper Benue Basin, N.E. Nigeria. Rev. Micropaleontol vol. 29(1), pp. 61-83.

Majumdar RK, Das D (2011). Hydrological Characterization and Estimation of Aquifer Properties from Electrical Sounding Data in Sagar Island Region, South 24 Parganas, West Bengal, India. Asian J. Earth Sci. 4: 60-74.

Molindo WA, Alile OM (2007). Evaluation of the Thermal Conductivity of Soils in Edo State, Nigeria. J. Appl. Sci. 7: 519-522.

Mpanda S (1997). Geological development of East African coastal basin of Tanzania: Acta Universities Stockholmiensis, v. 45, 121p.

Nton ME, Elueze AA (2005). Compositional characteristics and industrial assessment of sedimentary clay bodies in part of Eastern Dahomey basin, Southwestern Nigeria. Journal of Mining and Geology. 412 Pp. 175 -184.

Nton, ME (2001). Sedimentological and geochemical studies of rock units in the eastern Dahomey basin, south western Nigeria, unpublished P.H.D thesis, University of Ibadan, pp 315.

Nwankwo LI (2011). 2D Resistivity Survey for Groundwater Exploration in a Hard Rock Terrain: A Case Study of MAGDAS Observatory, UNILORIN, Nigeria. Asian J. Earth Sci. 4: 46-53.

Ogala JE, Ola-Buraimo AO, Akaegbobi IM (2009). Palynological investigation of the Middle- Upper Maastrichtian Mamu Coal facies in Anambra Basin, Nigeria. World Appl. Sci. J. vol. 7, n. 12, p. 1566-1575.

Ojeda HA (1982). Structural framework, stratigraphy, and evolution of Brazilian basins. AAPG Bull. v. 66, p.732-749.

Omatsola, ME, Adegoke OS (1981). Tectonic evolution and Cretaceous stratigraphy of the Dahomey basin. Nigeria Journal Mining and Geology 18 (01), 130–137.

Rosendahl BR (1987). Architecture of continental rifts with special reference to East Africa: Annual Review of Earth and Planetary Science, v. 15, p. 445-503.

Schlische RW (1991). Half-graben filling models: New constraints on continental extensional basin development: Basin Research, v. 3, p. 123-141.

Sirhan AM, Hamidi, Andrieux P (2011). Electrical resistivity tomography, an assessment tool for water resource: Case study of Al-Aroub Basin, West Bank, Palestine.. Asian J. Earth Sci., 4: 38-45.

Steeples DW (2001). Engineering and environmental geophysics at the millennium. Geophysics 66(1), 31-35

Storey BC (1995). The role of mantle plumes in continental breaks up: case history from Gondwanaland – Nature, v. 377, p. 301-308.

Suzuki K, Toda S, Kusunoky K, Fujimitsu Y, Mogi T, Jomori A (2000). Case studies of electrical and electromagnetic methods applied to mapping active faults beneath the thick Quaternary, Engineering Geology 56, 29-45

Unsworth MJ, Egbert G, Booker J (1999) High Resolution electromagnetic imaging of the San Andreas fault in Central California. Journal of Geophysical Research 104, 1131-1150.

Vail PR, Mitchum, RM, Thompson, S (1977). Seismic stratigraphy and global changes of sea level, Part 4: global cycles of relative changes of sea level. In: Payton, C.E (Ed.), Seismic Stratigraphy-Applications to Hydrocarbon Exploration, Am. Assoc. Petrol. Geol. Mem. 26, 83-97.

Van Wagoner JC, Mitchum RM, Campion KM, Rahmanian,VD (1990). Siliciclastic sequence stratigraphy in well logs, cores, and outcrop. Am. Assoc, Petrol. Geol. Methods Exploration Series 7.

White RS, Mckenzie DP (1989). Magmatism at rift zones: the generation of volcanic continental margins and flood basalts. J. Geophy. Res. 94, 7685-7729.

Yunus LE, Alper D, Can E (2008). Delineation of the Seawater-Freshwater Interface from the Coastal Alluvium of Kalekoy-Gokceada, NW Turkey. J. Appl. Sci. 8: 1977-1981.